When conventional methods fall short: identification of invasive cryptic Golden Apple Snails (Pomacea canaliculata; P. maculata) using environmental DNA

Banerjee, P.; Stewart, K.A.; Dey, G.; Sharma, R.K.; Maity, J.P.; Chan, M.W.Y.; ... ; Chen, C.-Y.

Check for updates

When conventional methods fall short: identification of invasive cryptic Golden Apple Snails (*Pomacea canaliculata*; *P. maculata*) using environmental DNA

Pritam Banerjee · Kathryn A. Stewart · Gobinda Dey · Raju Kumar Sharma · Jyoti Prakash Maity ·
Michael W. Y. Chan · Kuo Pin Chang · Tsung-Hsien Chen · Chia-Ti Hsu · Chien-Yen Chen

Abstract Cryptic invasions are difficult to distinguish and easily overlooked by conventional identification methods, creating false biodiversity information. Molecular markers represent the only reliable method to distinguish cryptic species to date but require individual tissue samples, which is time-inefficient and difficult during low abundance or early colonization. Newly developed Environmental DNA (eDNA) methods may provide a solution. We compared conventional methods (morphological, physicochemical) and molecular methods (DNA and eDNA) to distinguish two putative species of *Pomacea*, with the aim to develop an early taxon-specific detection method for effective invasive species management. Novel eDNA methods were assessed in semi-natural (mesocosm) and natural waterbodies across Taiwan for species identification. Morphological characters and physicochemical analysis of *P. canaliculata* and *P. maculata* shells demonstrated overlapping

Handling editor: Xavier Pochon

Supplementary Information The online version contains supplementary material available at https://doi.org/10.1007/s10750-022-04979-6.

P. Banerjee · G. Dey · M. W. Y. Chan
Department of Biomedical sciences, Graduate Institute
of Molecular Biology, National Chung Cheng University,
168 University Road, Min-Hsiung, Chiayi County 62102,
Taiwan

P. Banerjee · G. Dey · R. K. Sharma · J. P. Maity ·
C.-T. Hsu · C.-Y. Chen (✉)
Department of Earth and Environmental Sciences,
National Chung Cheng University, 168 University Road,
Min-Hsiung, Chiayi County 62102, Taiwan
e-mail: chien-yen.chen@oriel.oxon.org; yen@eq.ccu.edu.tw

K. A. Stewart
Institute of Environmental Sciences, Leiden University,
2333 CC Leiden, The Netherlands

R. K. Sharma
Department of Chemistry and Biochemistry, National
Chung Cheng University, 168 University Road,
Min-Hsiung, Chiayi County 62102, Taiwan

J. P. Maity
Environmnetal Science Laboratory, Department
of Chemistry, School of Applied Sciences, KIIT Deemed
to be University, Bhubaneswar, Odisha 751024, India

K. P. Chang (✉)
Department of Ophthalmology, Ditmanson Medical
Foundation Chiayi Christian Hospital, Chiayi City, Taiwan
e-mail: kbc2603@gmail.com

T.-H. Chen
Department of Internal Medicine, Ditmanson Medical
Foundation Chiayi Christian Hospital, Chiayi City, Taiwan

C.-T. Hsu
Concordia High School, 621 No. 31, Section 2, Jianguo
Road, Minxiong Township, Chiayi, Taiwan

C.-Y. Chen
Center for Nano Bio-Detection, Center for Innovative
Research on Aging Society, AIM-HI, National Chung
Cheng University, Chiayi 62102, Taiwan

qualitative and quantitative measures, which were unable to differentiate species. However, DNA-based barcoding (COI gene) differentiated *P. canaliculata*, and *P. maculata* and revealed their distribution. Our eDNA analysis demonstrated overall detection rate of *P. canaliculata* was significantly higher than *P. maculata*. Importantly, we detected the active presence of *P. maculata* in Taiwan, although further studies investigation needed to differentiate pure and hybrids individuals. This pioneering eDNA study quickly and effectively detected *P. canaliculata* and *P. maculata*, which could revolutionize tracking two immensely invasive and economically destructive species.

Introduction

Invasive alien species (transported and established non-natives) pose extreme threats to the areas to which they are introduced, by creating an imbalance in the natural ecosystem, carrying disease, and eliminating local populations (Tobin, 2018; Shabani et al., 2020). While the negative impacts on local biodiversity caused by these invasive species can be overcome through directed preventative mitigation and remediation measures (Pyšek & Richardson, 2010; Venette et al., 2021), this requires proper taxonomic identification coupled with fast and effective detection and management decisions (Tobin, 2018). In cases involving cryptic invasions where observational and morphological identification/distinction are each difficult or error-prone, invasive species that are undetected or misidentified can lead to false biodiversity information (Ramos et al., 2020), thus making species-specific management approaches ineffective and their knock-on effects difficult to understand.

Arguably, amongst the world's most destructive invasive pests are snails of the genus *Pomacea* (Naylor, 1996; Lowe et al., 2000), which were first introduced to East and South–East Asia during the 1980's for dietary protein supplementation and commercial utilization (Wu et al., 2011). Subsequently, *Pomacea* spp. (sometime referred to as 'Golden Apple

Snails') were identified as species of serious concern due to their destruction to local agriculture [e.g., reduced rice production; (Naylor, 1996)], spreading of life-threatening diseases [e.g., intermediate host of *Angiostrongylus cantonensis*; (Lv et al., 2018)], and outcompeting native populations with their high reproduction rate, fast growth, lack of natural enemies, and ability to tolerate various environmental stresses (Liu et al., 2018). Although some *Pomacea* spp. have been utilized for food, agricultural, medicinal, and other economic benefits (Laonapakul et al., 2019), their widespread environmental destruction continues to make their identification, utilization (waste-to-wealth), and removal, a top priority.

Making matters worse, different *Pomacea* spp. have been introduced multiple times, and due to their lack of morphological distinction (Thiengo et al., 1993; Cazzaniga, 2002), it is persistently difficult to identify closely related species (Rama Rao et al., 2018). In fact, two cryptic invasive *Pomacea* spp. (i.e., *Pomacea canaliculata*, and *P. maculata*), are considered particularly onerous to distinguish by conventional taxonomists. Conventional taxonomy of *Pomacea* spp. is generally based on snail-shell properties, egg mass, and soft tissue morphology; however, field identification and differentiation of *P. canaliculata* and *P. maculata* based on these characters remains a challenge. In addition to this, conventional methods are time-consuming and hard to accomplish in the field (Matsukura & Wada, 2017). Indeed, their similar morphological characteristics and limited genetic differentiation lead to frequent misidentification (Yang et al., 2018).

The successive failure of conventional monitoring to get satisfactory results from spot-identification and visual discrimination has recently led to the utilization of DNA-based methods, where molecular markers (especially mitochondrial COI) are used to determine species based on their genetic differences (Yang et al., 2018). Other recognized markers [e.g., (Inter Simple Sequence Repeat; ISSR), mitochondrial rRNA (Rawlings et al., 2007; Matsukura et al., 2008), 18S rDNA, histone 3 subunit, and EF1α (Hayes et al., 2009)] have also recently been used to successfully distinguish *Pomacea* spp. (Matsukura & Wada, 2017). Furthermore, the use of Environmental DNA or "eDNA" has provided a promising non-invasive/

non-destructive approach for quick monitoring (Taberlet et al., 2012; Banerjee et al., 2021). In fact, monitoring approaches using eDNA based methods have gained popularity amongst ecologists, conservation biologists, and wildlife managers as it generally: (i) does not require direct observation or handling of organisms (Taberlet et al., 2012). This approach thus provides detection (presence/absence), relative abundance, distribution, and even species interaction data in a fast, cheap, and non-invasive manner (Qu & Stewart, 2019; Banerjee et al., 2021); (ii) is found to be equally (or more) accurate as compared to conventional methods for various species (Kuzmina et al., 2018)—especially in circumstances of low abundance, extreme habitats, phenotypic plasticity, juvenile stages, and during the early stages of invasion; and (iii) records a higher diversity of taxa in a single sampling than morphological and DNA-based (tissue samples) methods (McElroy et al., 2020; Fediajevaite et al., 2021). In fact, eDNA-based methods are well known for detecting invasive species early during colonization (Ficetola et al., 2008), and recent optimization/standardization practices have improved their accuracy for more reliable detection of targeted species, reinforcing eDNA's trustworthiness for field applications (Deiner et al., 2021). Therefore, eDNA methods could revolutionize how we survey the distribution, abundance, and interactions of cryptic and invasive *P. canaliculata*, and *P. maculata* in nature.

Here, the present study compares the use of three different approaches to identify, differentiate and reduce the false identification of (putative) *P. canaliculata* and *P. maculata*: (i) morphologically screening *P. canaliculata* and *P. maculata* sensu previous studies (Matsukura et al., 2008; Rama Rao et al., 2018), (ii) physicochemical differentiation methods as an alternative approach to discriminate between the two cryptic invasive snail species, and (iii) genetic approaches, including the development of a cost-effective, non-invasive eDNA-based monitoring method with the aim of a new framework for invasion management of *Pomacea* spp. Our study focuses on Taiwan, wherein the distribution of *Pomacea* spp. currently encompasses agricultural fields, wastewater drainage, and reservoirs across the country (Wu et al., 2010). To date, only *Pomacea canaliculata* [introduced in 1980; (Wu et al., 2010)] has been noted within Taiwan, but it has recently been suggested that

P. maculata may be currently present within the country but misidentified with *P. canaliculata* due their cryptic similarity and lack of molecular method implementation (Hayes et al., 2008). Thus, the detailed distribution of *P. canaliculata* and *P. maculata* is still yet to be critically evaluated, which has stunted effective invasive remediation. By delineating the best practices for identifying *Pomacea* spp., we aim to understand the species-specific effects and aid in mitigating their invasive spread and economic damage.

Materials and methods

Snail sample collection and preparation

Pomacea spp. were collected (10–15 individuals from each site) from rice fields, and agricultural drainage during three sampling events occurring in September 2020, January, and March 2021 from Minxiong, Chiayi county, Taiwan (supplementary Table 1). In addition, Giant African Snail (*Lissachatina* sp.) samples were collected from National Chung Cheng University (Minxiong, Taiwan) campus on the same date to use as a control (for eDNA-based mesocosm experiment). The snails were transported to the laboratory, thereafter washed (with brush and distilled water to remove debris), and isolated in separate aquariums (according to the sampling site). Subsequently, experiments proceeded with three treatments: (i) mesocosm study for eDNA, where mature snails were placed in aquariums and were incubated for 7 days before the collection of water samples, (ii) morphological measurements were collected based on visible taxonomic characters, and (iii) physicochemical analysis and DNA barcoding, where 30 snails were heat-shocked using a microwave oven and the inner tissue was removed using sterile forceps. Snail tissues were subjected to DNA extraction and preservation for further experiments, and the shells were cleaned thoroughly, again using a 10% sodium hypochlorite solution followed by distilled water. Shells were then left to dry in a hot-air oven (JA-72) at 65°C for 24 h. Afterward, each shell was individually ground into a fine powder using a mortar and pestle, then placed in a 2 ml microcentrifuge tube for further physicochemical analysis. Tissues and shells from each individual were marked with the same sampling number.

Identification and discrimination of *Pomacea* spp. with conventional methods

Investigation of morphological crypsis of Pomacea spp.

We measured *Pomacea* spp. based on morphologically distinguishable quantitative and qualitative shell characters as described by others (Matsukura et al., 2008; Rama Rao et al., 2018). Using the Vernier caliper scale (±0.02 mm), we measured shell height, width, weight, spire height, aperture height, and aperture width, in addition to noting pallial leaf pigmentation, shell surface, thickness, and shoulder shapes (Rama Rao et al., 2018). As morphological characters of these snails are reported to be highly variable and overlapping, all data were taken by the same person to minimize interindividual measurement error. We further observed the transverse section of snail shells under the Field Emission Scanning Electron Microscope (FE-SEM; Hitachi S4800-I instrument, Japan).

Investigation of physicochemical crypsis of *Pomacea* spp.

Detection of crystalline structure of snail shell with X-ray powder diffraction (XRD)

X-ray powder diffraction (XRD) is often the method of choice for accurate detection of molecular structure at an atomic resolution (Chauhan & Chauhan, 2014; Sharma et al., 2021) and has the potential to solve the structure of arbitrary molecules/crystallized minerals. Crystallographic information obtained from XRD is used in different fields, such as electronic devices, mineralogy, geoscience, material science, pharmaceutical, characterization of biological macromolecules, environmental and forensic sciences, etc. (Aitipamula & Vangala, 2017).

The shell powders of *Pomacea* spp. were analyzed at room temperature using wide-angle XRD following the method described by Maity et al., (2019). The XRD diffraction pattern was operated through Scintillation Counter Detector (Bruker MeaSrv-D2-205680 PHASER instrument, $\lambda = 1.540600$ nm) at the scan rate of 2°C per min, elevated temperature from the 2θ range of 10°–70° with their step size 0.020135, where the Ni-filtered Cu Kα radiation was used at operating temperature 10 mA and voltage 30 kV to detect the XRD patterns. The crystalline structure, phase composition, and physical properties analyzed through XRD were used to understand the cryptic nature of *P. canaliculata* and *P. maculata* shells.

Detection of characteristic functional groups with Fourier-transform infrared spectroscopy (FTIR)

Fourier-transform infrared spectroscopy (FTIR) is a fast and cost-effective method to characterize chemical properties and identify the presence of functional groups based on different vibration modes at different infrared wave numbers (Valand et al., 2020; Sharma et al., 2021). The presence or absence of functional groups of protein, lipids, and carbohydrates can help to identify bacteria (Ojeda & Dittrich, 2012; Maity et al., 2013), and is now being applied to higher organisms (Kenđel & Zimmermann, 2020).

The FTIR spectra were performed using liquid-nitrogen-cooled mercury–cadmium–telluride (MCT) detector (FTIR, FTIR Bruker optics-2141 Vertex-70V in RT-DLaTGS sample compartment), followed by the procedure of Maity et al., (2013). The functional groups of snail shell powder were estimated using KBr powder (KBr/sample weight ratio = 20:1) in the range of 4000–400 cm^{-1}. The peak position, baseline correction, and smoothing were performed automatically by peak resolve (Thermo-Fisher-Nicolet, OMNIC 7.1). All samples were analyzed using Spectrum software (PerkinElmer V5.0) and Knowitall software (Bio-redIR/NIR Edition) (Liu et al., 2013; Maity et al., 2013). The chemical composition was noted through the presence of functional groups in the shell of *P. canaliculata* and *P. maculata.*

Detection of characteristic functional groups with Raman spectroscopy

Raman spectroscopy/imaging is a technique using the intensity and frequency of monochromatic light to aid in identifying biochemical fingerprints, where identification, discrimination, and differentiation of a cell, tissue, or organism are performed successively (Jones et al., 2019).

Raman spectra of powdered snail shells were recorded using RAMaker (ProTrustTech). The samples were illuminated by a COM laser (Lambda beam PB, 53-100 DPSS) line at 532.267 nm wavelength with a power of 101 mW. The spectrum was recorded

in the region of 100–3000 cm^{-1} with a range at resolution of 2 cm^{-1} and 3 scans per point. The collected spectra were processed using RAM Spec software for Andor V1.1.0 (Build 20161218) to understand the chemical composition (especially fingerprints) of the shell of *P. canaliculata* and *P. maculata*.

FE-SEM–EDS analysis

The chemical analysis of powdered snail shell material was conducted using Field Emission-Scanning Electron Microscope (FE-SEM; Hitachi S4800-I instrument, Japan) equipped with an Energy Dispersive Spectroscopy (EDS), where a carbon-taped aluminum plate as a holder, the accelerating voltage 0.1–30 kV with magnification: 30~800,000X was estimated using cold-cathode electron gun as emission source and vacuum sputtered coated with gold.

Identification and discrimination of *Pomacea* spp. with molecular methods

DNA barcoding

DNA was extracted from 35 individual snail samples (30 unknown species of *Pomacea*, and 5 *Lissachatina* sp.) that occupied the mesocosms with the help of DNeasy blood & tissue kit (Qiagen). In general, 20–50 mg of tissue was removed from the foot muscle of the snail and chopped into small pieces to avoid contamination of any parasite; the rest of the tissues were stored in ethanol (70%) and kept at − 20°C. Tissue samples were added to 180 µl of ATL lysis buffer and 20 µl Proteinase K, which were then incubated in a dry bath (at 56°C) until complete lysis. Further steps were performed according to the manufacturer's protocol with a final volume of elution of 100 µl. Mitochondrial COI primers were used to distinguish *Pomacea* spp. based on putitative sequence differences. First, we amplified snail DNA (*Pomacea* spp., and *Lissachatina* sp.) with LCO1490 (5′ GGT CAA CAA ATC ATA AAG ATA TTG G-3′) and HCO2198 (5′ TAA ACT TCA GGG TGA CAA AAA AAT CA-3′) primers (Vrijenhoek, 1994), and subsequently used species-specific primers for *Pomacea* spp.: PcanCOI (F) (5′-TGG GGT ATG ATC AGG CC-3′) and PinsCOI (F) (5′-ATC TGC TGC TGT TGA AAG-3′) and HCO2198 (R) (5′-TAA ACT TCA GGG TGA CCA AAA AAT CA-3′) developed by

Matsukura et al., (2008). These primers were validated in silico with the help of NCBI Primer Blast (https://www.ncbi.nlm.nih.gov/tools/primer-blast/) and later checked using PCR with *Lissachatina* sp. as a negative control. PcanCOI (F) targets *Pomacea canaliculata* (666 bp amplicon) and PinsCOI (F) targets *Pomacea maculata* (390 bp amplicon) with the help of a common reverse primer HCO2198 (R). To compare the detection efficiency of shorter PCR products and longer PCR products (Ma et al., 2016), we designed an additional primer with the help of a previous tissue-derived DNA amplified sequence. The newly designed primers PomaCF (F) (5′-TGG GGT ATG ATC AGG CC-3′), PomaMF (5′-TGG AGT ATG ATC AGG TT-3′) and PomaR—(5′-CCA AAT CCA CCA ATT ATT ATA G-3′) can amplify 171 bp product and are species-specific. Furthermore, we performed in silico PCR with the help of NCBI primer BLAST (https://www.ncbi.nlm.nih.gov/tools/primer-blast/), and also checked the specificity of our primer with closely related taxa (taxonomic list in Table S3). We tested our primer in the laboratory, where we performed separate amplification of PcanCOI with PomaR and PomaMF with PomaR for *P. canaliculata* and *P. maculata* as positive samples, and *Lissachatina* sp., as a negative sample.

Conventional PCR was performed using the CUL-BIO PCR system with 96-well temperature gradient PCR (CB series). A final reaction mixture (25 µl) was prepared using: 5×Fast-RunTM *Taq* Master Mix with Dye (5 µl) (Protech), 10 pmol forward and reverse primers (0.5 µl each) (genomics, Taiwan), DNA from tissue sample (1 µl), and final volume makeup was done using high quality, sterile, distilled water. The extracted DNA from the tissue sample was amplified with an initial denaturation of 5 min at 94°C followed by a continuous 36 cycles of amplification with denaturation of 30 s at 94°C, annealing of 30 s at 55°C for PanCOI, PinsCOI and HCO2198 and 60°C for PomaCF, PomaMF, PomaR, and extension of 1 min at 72°C. After completing 36 cycles, the final extension was at 72°C for 5 min (Matsukura et al., 2008; Rama Rao et al., 2018).

eDNA barcoding

Mesocosm Five aquariums containing 3 l of tap-water each, were set up to conduct mesocosm experiments. In three aquariums, ten *Pomacea* spp. (unknown spe-

Fig. 1 Location of eDNA field sampling sites for *Pomacea* spp., conducted during June to September, 2021
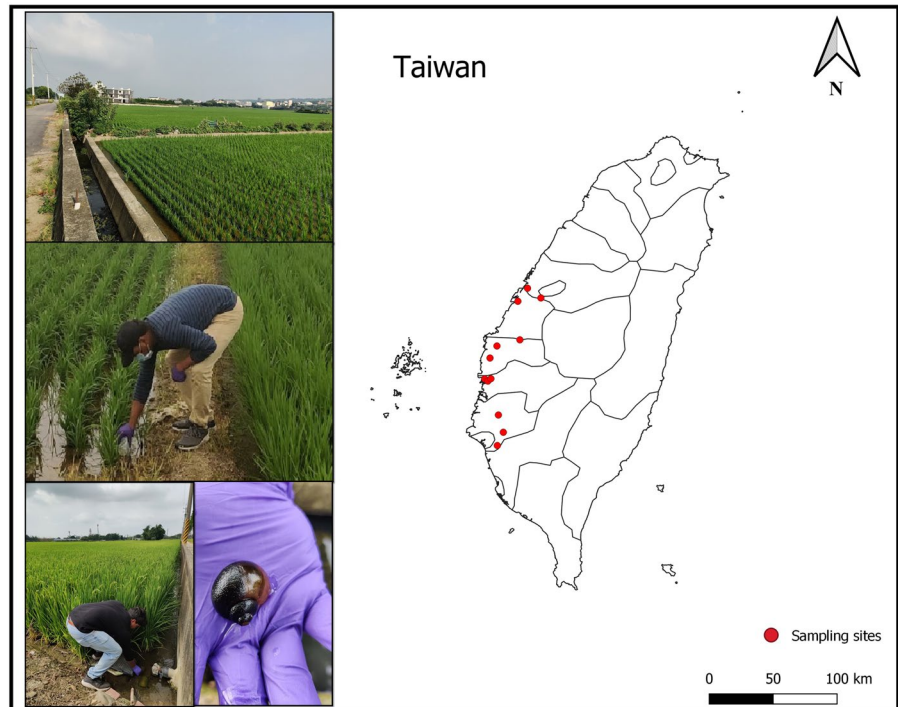
cies) for total biomass equaled ~ 60 g (weighed prior to experimentation). In another aquarium, we placed five Giant African Land Snails (*Lissachatina* sp.), and the fifth aquarium contained no snail DNA throughout the study, these aquariums were used as a negative control. After 7 days of incubation, three replicates of 300 ml of water were taken from each aquarium with the help of a previously cleaned (once with 10% bleach then two times with distilled water) plastic bottles. The mesocosm study was carried out three times according to sample collection date (September 2020, January 2021, March 2021), with all samples acquired in triplicate.

Field sampling   The eDNA method was validated by conducting field surveys from four counties of Taiwan (Chiayi, Changhua, Tainan, Yunlin; Fig. 1, Supplementary Table 1) during June to September 2021. The climatic condition in the sampling zones can be summarized as hot, humid, and wet, with an average temperature of 29°C. During sampling, 500 ml of water was collected with sterilized bottles (in triplicate) from three different locations in each county (Table 3). After collection, the bottles were placed on ice and taken to the laboratory within 3–5 h. One col-

lection blank (deionized water) was taken at each sampling site to evaluate contamination (false detection) during field collections.

Laboratory analysis

After the collection (Mesocosm and field), samples were filtered through sterile 47-mm diameter and 0.45 μm pore size filter paper (GN-6 Metricel ®, Pall Corporation) (Bruce et al., 2021). In every filtration process, one blank sample containing distilled water was filtered to assess contamination and false positives at the laboratory (Bruce et al., 2021). After filtration, half of the filter paper was stored in 75% ethanol for further use, and from the other half, eDNA extraction was immediately done. The eDNA from the filter paper was extracted using DNeasy Blood & Tissue kit (Qiagen) following the manufacturer's protocol, where modification was done in the following steps: the filter paper was incubated (60°C) overnight in a mixture of 180 μl of ATL lysis buffer and 20 μl Proteinase K, and final volume of elution buffer was 50 μl. The eluted DNA was stored at − 20°C. The Limit of detection (LOD) was analyzed after serial dilution of a positive DNA sample with a known concentration as well as a non-target DNA sample (*Lissachatina* sp.) (Chandrashekhar et al., 2015).
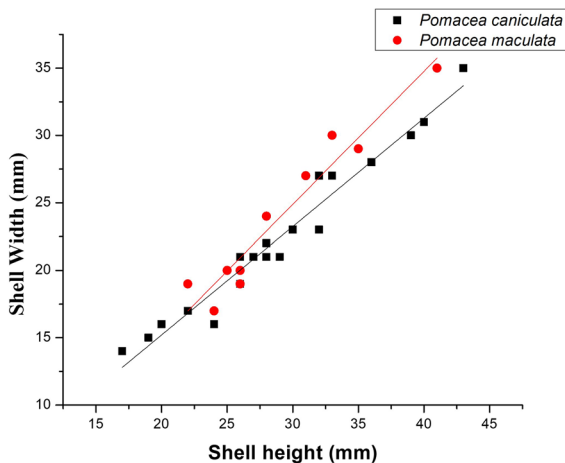
Fig. 2 Correlation of snail shell height (mm) and width (mm) of *P. canaliculata* (*N* = 20) and *P. maculata* (*N* = 10)

In conventional PCR final reaction mixture of 25 µl was prepared using: 5×Fast-RunTM *Taq* Master Mix with Dye (5 µl) (Protech), 10 pmol forward and reverse primers (0.5 µl each) (genomics, Taiwan), eDNA sample (4 µl), and final volume makeup was done using high quality, sterile, distilled water. The cPCR conditions were the same as DNA barcoding (see the previous section on tissue DNA barcoding) except 45 cycles for amplification. The PCR products were run on a 1.5% agarose gel with 100 bp ladder (Protech). All amplified PCR products (tissue samples and eDNA samples) were sent to Mission Biotech Co., Ltd, Taiwan for sequencing in both directions. All the sequences were confirmed in Chromas 1.0 and Bioedit and aligned using the CLUSTAL X program.

Results

Identification and discrimination of *Pomacea* spp. with conventional methods

Investigation of morphological crypsis of Pomacea spp.

Shell height had a significant relationship with shell width, spire height, aperture height, aperture width, and shell weight (Fig. 2, Supplementary data 2). Comparing quantitative characters of *P. canaliculata* and *P. maculata*, shell width showed the most differentiation (Table 1, Fig. 2), where *P. maculata* was wider (25.20 ± 1.89) compared to *P. canaliculata* (22.88 ± 1.16). However, all quantitative characters showed no significant difference between the species (Table 1), corroborating the claim of their morphological crypsis. Furthermore, we found qualitative characters were also highly variable and not diagnostic to species (Fig. 3). The shell ultrastructure of both the species showed three distinctive layers, a blocky or pillar-like prismatic layer, followed by a cross lamellar layer, then a short nacreous layer (Fig. 4). In short, all morphological characters were found to be highly overlapping, with little taxonomic resolution.

Investigation of physicochemical crypsis of *Pomacea* spp.

Detection of the crystalline structure of snail shell with X-ray powder diffraction (XRD)

The crystallinity of raw cryptic *P. canaliculata* and *P. maculata* was compared using X-ray powder diffraction (XRD) and the peaks at 26.19°/26.23° and

Table 1 Comparison of potential morphological diagnostic quantitative characteristics of *Pomacea* spp.; *P. canaliculata* (*N* = 20) and *P. maculata* (*N* = 10)

Quantitative characters	P. canaliculata	P. maculata	t value	P value
Shell height (mm)	29.78 ± 1.37	30.10 ± 1.84	0.13	0.45
Shell Width (mm)	22.88 ± 1.16	25.20 ± 1.89	1.06	0.15
Spire height (mm)	6.60 ± 0.29	6.80 ± 0.42	0.38	0.35
Aperture height (mm)	18.23 ± 0.62	18.15 ± 1.01	0.06	0.47
Aperture width (mm)	13.35 ± 0.54	13.20 ± 0.61	0.17	0.44
Snail mass (g)	7.45 ± 0.44	8.24 ± 0.63	1.01	0.16
Shell mass (without tissue) (g)	1.56 ± 0.11	1.28 ± 0.16	1.39	0.09

Fig. 3 Comparison of qualitative characters (based on observation) of *P. canaliculata* and *P. maculata*
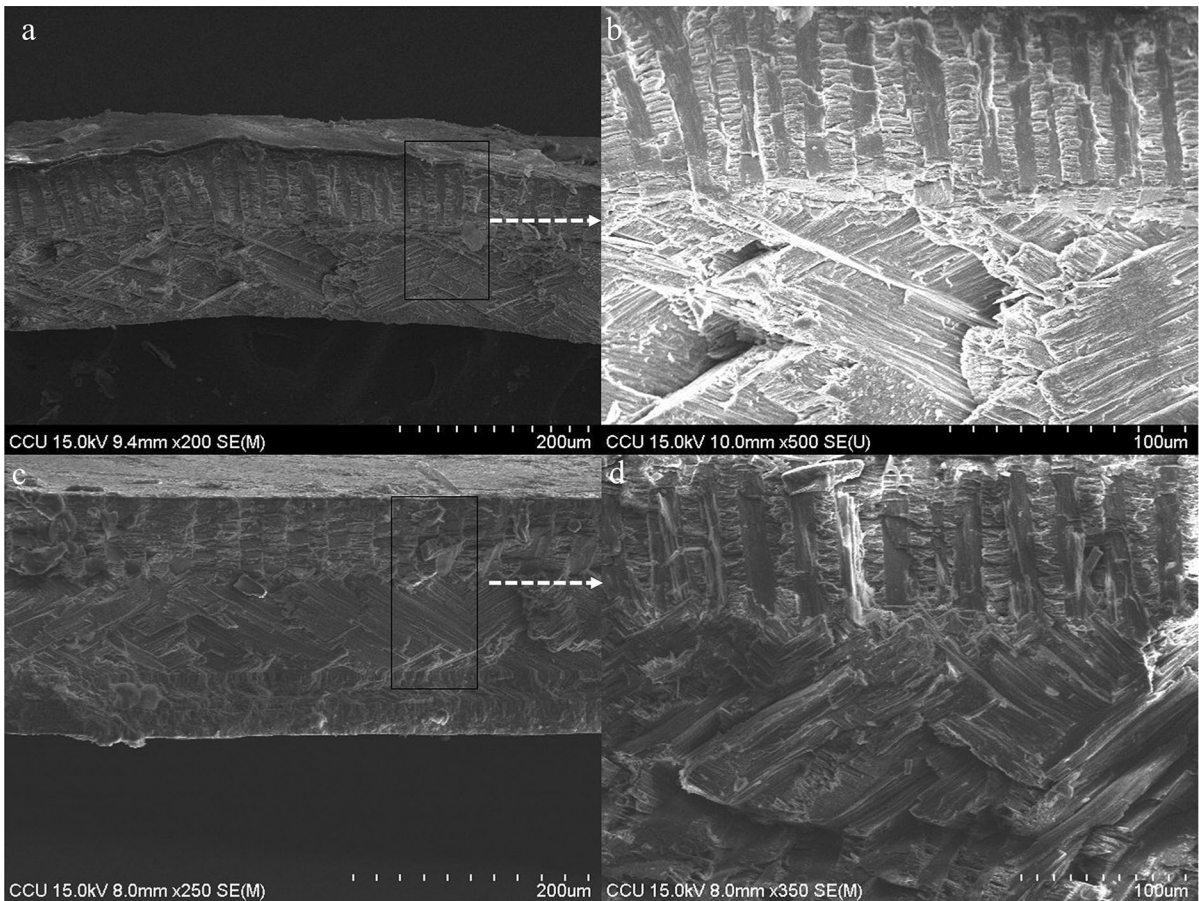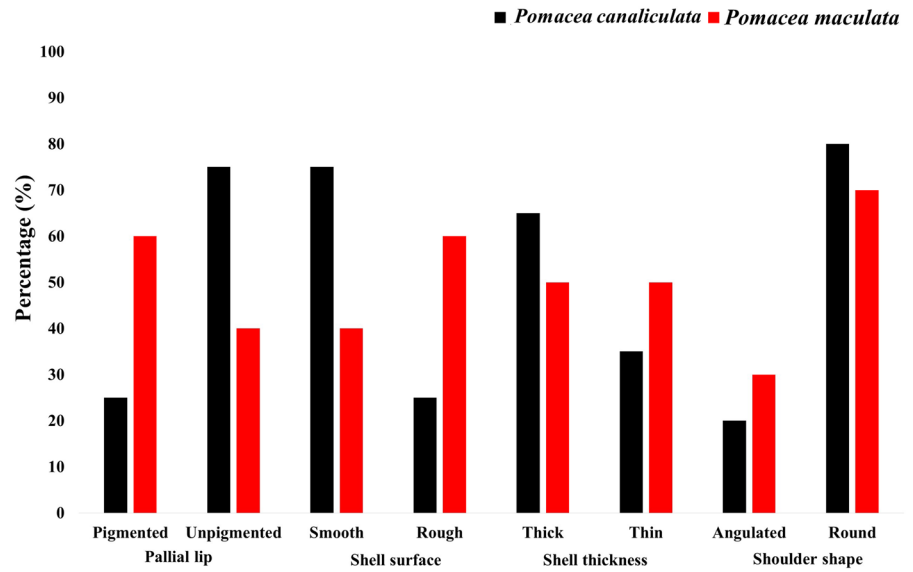

Fig. 4 Transverse section exemplar of *Pomacea* spp. showing the internal structure of *P. canaliculata* (**a** 200 µm and **b** 10 nm) and *P. maculata* (**c** 200 µm and **d** 10 nm)
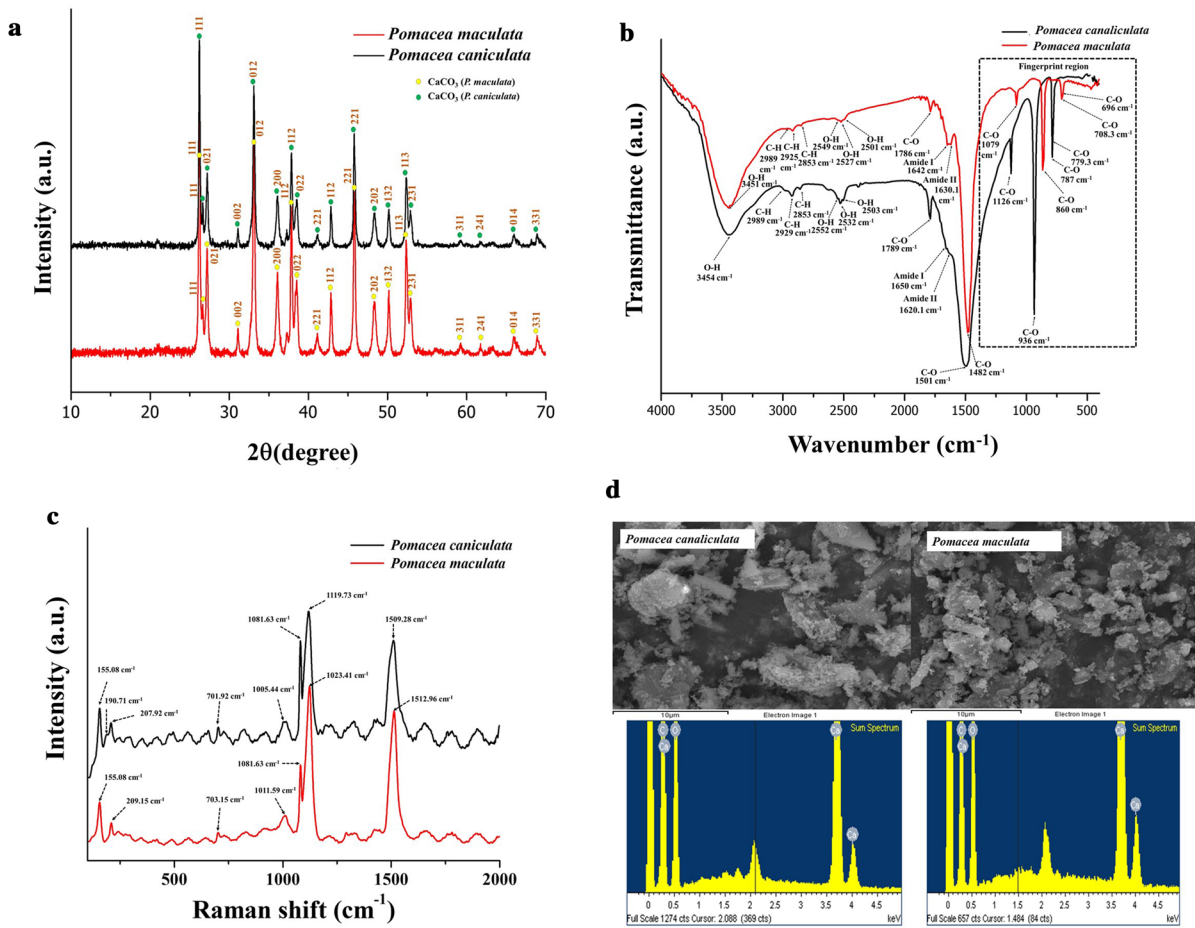
Fig. 5 Investigation of physicochemical crypsis of *Pomacea* spp. **a** X-ray diffraction (XRD) **b** Fourier-transform infrared spectroscopy (FTIR), **c** Raman spectra, **d** FE-SEM–EDS anal-ysis of raw *Pomacea* spp. shell [*Pomacea canaliculata* ($N=3$) and *Pomacea maculata* ($N=3$)]

26.66°/27.19° corresponding to (111), (021) miller index, respectively, which is indexed as $CaCO_3$ (Fig. 5a). This result provides evidence of the existence of the orthorhombic aragonite phase of $CaCO_3$ in both the snail shells. The intensity peak and Miller indices corresponding to the peaks of *P. canaliculata* and *P. maculata* were found to be similar.

Detection of characteristic functional groups with Fourier-transform infrared spectroscopy (FTIR)

The infrared peaks of *P. canaliculata* and *P. maculata* were compared (Fig. 5b), which confirmed the band corresponding to 1,789/1,786, 1,501/1,482, 936/860, 787/779, 708/696 cm^{-1} (*P. canaliculata*/*P. maculata*) are the absorption bands of CO_3^{2-} ions in $CaCO_3$

(Udomkan & Limsuwan, 2008; Parveen et al., 2020). The bands range from 3,300 to 3,500 cm^{-1} in correspondence to –OH stretching. In *P. canaliculata*/*P. maculata*, amide I, and amide II bands are found 1,650/1,642 cm^{-1} and 1,620/1,630 cm^{-1}, respectively. The bands at 2,989/2,989, 2,925/2,929, 2,853/2,853 cm^{-1} appeared due to the CH$_2$ stretching of aliphatic chains (Parveen et al., 2020). The –OH was found in the range of 2,500–2,600 cm^{-1} due to the organic matter of the shell. In the fingerprint region, a signature of CO_3^{2-} ions in $CaCO_3$ was visible, where carbonate υ4 bands of aragonite were at 787/708 and 779/696 cm^{-1} and υ2 bands of aragonite at 963/860 cm^{-1}; justifying the presence of aragonite in both of the snails (Jovanovski et al., 2002; Vagenas et al., 2003; Parveen et al., 2020). The bands at

$1,501/1,482$ cm^{-1} and $1,079/1,126$ cm^{-1} correspond to υ3 and υ1 modes. Thus, the spectral analysis of *P. canaliculata* and *P. maculata* was also found to be almost indistinguishable.

Detection of characteristic functional groups with Raman spectroscopy

The Raman spectrum provided information about the presence of functional groups of snail shell powder of *P. canaliculata* and *P. maculata* (Fig. 5c). Two types of stretching (symmetric—600–1,200 cm^{-1} and asymmetric—1,200–1,700 cm^{-1}) of carbonate group $(CO_3)^{2-}$ are observed. The band present at $1,081$ cm^{-1} due to the υ1 symmetric mode of carbonate ions, and other bands such as 155–210 cm^{-1} are the lattice mode, $701/703$ cm^{-1} are the υ4 mode of carbonate ions (Harris et al., 2015; Borromeo et al., 2018). The existence of two bands at $1,119/1,123$ and $11,509/1,512$ cm^{-1} was observed due to single and double carbon–carbon bonds in the shell, signifying the presence of polyenes in the snail shell (Kupka et al., 2016; Komura et al., 2018). Raman spectrum analysis of both the species reveals similarities in intensity and position of bands.

Detection of characteristic chemical composition with FE-SEM–EDS analysis

FE-SEM–EDS was carried out for both species to understand any difference in chemical composition. The significant elements found Ca, O, C, and it was noticed that both the species have the same kind of chemical composition in the shell (Fig. 5d).

Identification and discrimination of *Pomacea* spp. with molecular methods

Detection of cryptic snails with DNA-based barcoding

Two invasive species of snails belonging to the genus *Pomacea* spp. were identified successfully with DNA-based barcoding methods (Fig. 6, Table 2). Amplification of *Pomacea* spp., and *Lissachatina* sp. (control) with LCO1490 and HCO2198 derived 650–680 bp amplicons, and sequencing of these fragments

confirmed their taxonomic identity (Fig. 6a). However, PCR multiplexing with species-specific primers PcanCOI (F) and PinsCOI (F), as well as reverse primer HCO2198 (R), amplified two characteristic length fragments in the case of *Pomacea* spp. (Matsukura et al., 2008; Rama Rao et al., 2018), and amplification of *Lissachatina* spp., was only found in the case of universal primers (LCO1490 and HCO2198; Fig. 6a). This corroborated the species-specificity of PcanCOI (F), PinsCOI (F), HCO2198 (R). The longer fragments (666 bp) amplified by species-specific primers were confirmed as *P. canaliculata* in the present study, which is comparable with previous reports (Matsukura et al., 2008; Rama Rao et al., 2018). The shorter fragments (390 bp), which were previously misidentified as *P. insularum* (Matsukura et al., 2008), and later confirmed as *P. maculata* (Rama Rao et al., 2018), were also found in the present study (Fig. 6). Furthermore, both amplified 171 bp products, POMACF and POMAR, were found to be specific for *P. canaliculata*, and POMAMF and POMAR were found to be specific for *P. maculata*. The limit of detection (LOD) was noted as ~6.84 picograms/µl (Supplementary Fig. 1). Using both of these primers, we detected *P. canaliculata* more frequently than *P. maculata* in all three sampling events. Out of 30 samples used for barcoding, 25 individuals were identified as *P. canaliculata* and 5 individuals were found to be *P. maculata* (Table 2).

Development of eDNA-based methods for rapid detection of *Pomacea* spp.

Performance in mesocosm

The eDNA samples collected from aquariums were successfully amplified with both sets of primers from almost every experimental mesocosm, where the mixture of *Pomacea* spp. were placed (Table 2). No amplified product was found from the two control aquariums (aquarium 4, with *Lissachatina* sp., and aquarium 5 with distilled water), in all three replicates. Both primers are similarly effective in terms of detection rate (Fig. 7). However, the detection rates via eDNA of both species differed significantly (Fig. 7, Table 2). *P. canaliculata* was detected
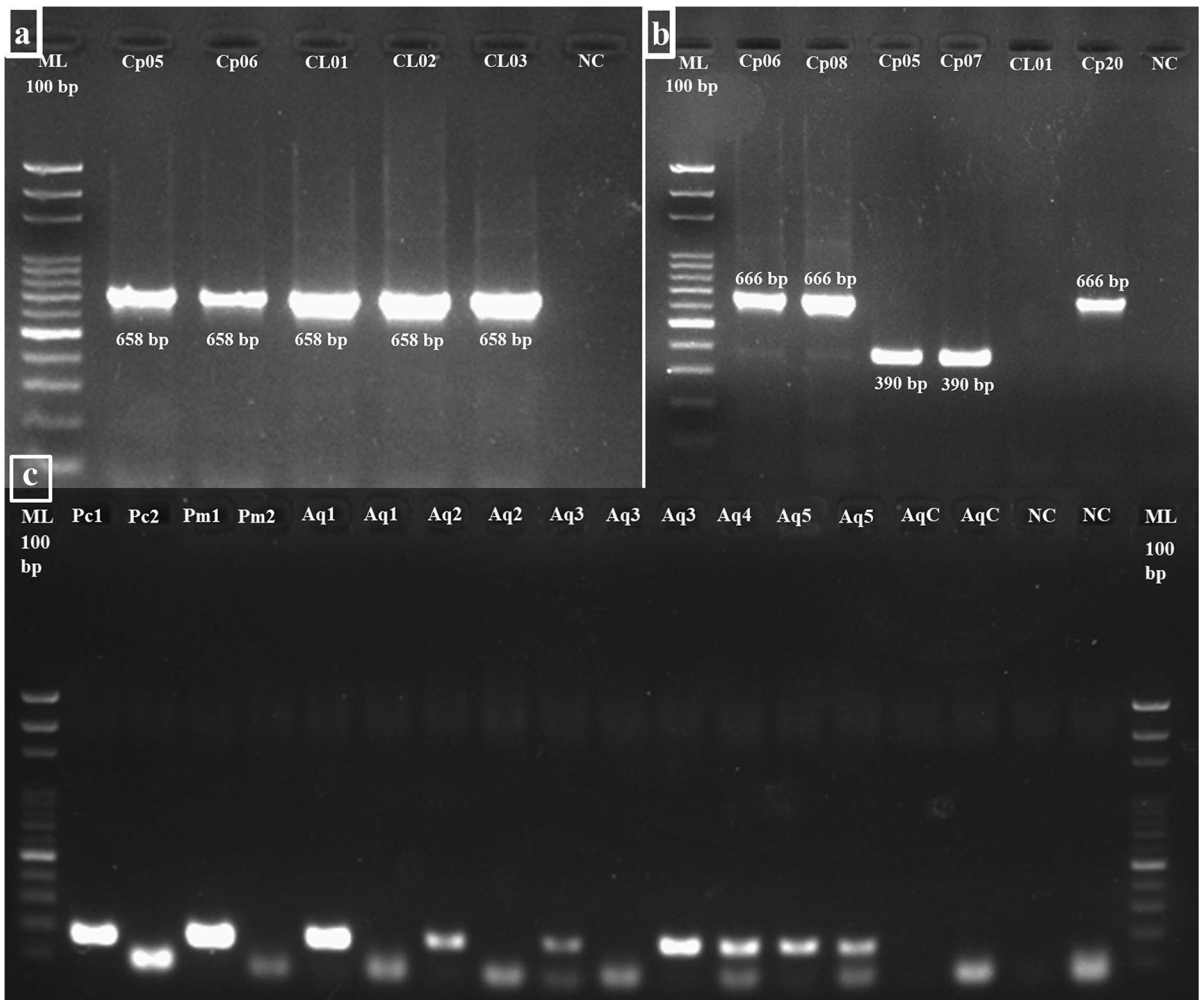
Fig. 6 Agarose gel electrophoresis image showing amplification of tissue derived from DNA barcoding and eDNA. **a** DNA amplification with universal primers LCO1490 and HCO2198, **b** species-specific primers PcanCOI, PinsCOI and HCO2198, and **c** eDNA with newly developed primers; Cp06, 08, 20: Pc1—*P. canaliculata*; Cp05, 07; Pm1—*P. maculata*; CL01-03—*Lissachatina* sp. Aq1-5—aquariums; Aq C—control aquarium; NC—negative control

Table 2 Detection rate of *P. canaliculata* and *P. maculata* with DNA barcoding and eDNA barcoding (mesocosm)

	Detection rate of PanCOI, PinsCOI and HCO2198		Detection rate of POMACF, POMAMF and POMAR	
	P. canaliculata	*P. maculata*	*P. canaliculata*	*P. maculata*
DNA barcoding				
Aquarium 1 (*Pomacea* sp.)	8/10	2/10	8/10	2/10
Aquarium 2 (*Pomacea* sp.)	9/10	1/10	9/10	1/10
Aquarium 3 (*Pomacea* sp.)	8/10	2/10	8/10	2/10
Aquarium 4 (*Lissachatina* sp.)	0/5	0/5	0/5	0/5
eDNA barcoding				
Aquarium 1 (*Pomacea* sp.)	2/3	2/3	3/3	2/3
Aquarium 2 (*Pomacea* sp.)	3/3	2/3	3/3	1/3
Aquarium 3 (*Pomacea* sp.)	3/3	1/3	3/3	1/3
Aquarium 4 (*Lissachatina* sp.)	0/3	0/3	0/3	0/3
Aquarium 5 (distilled water)	0/3	0/3	0/3	0/3

Fig. 7 Comparison of detection of *P. canaliculata* and *P. maculata* (using both primers, longer amplicon 666,390 and shorter amplicon 171) in mesocosm and field
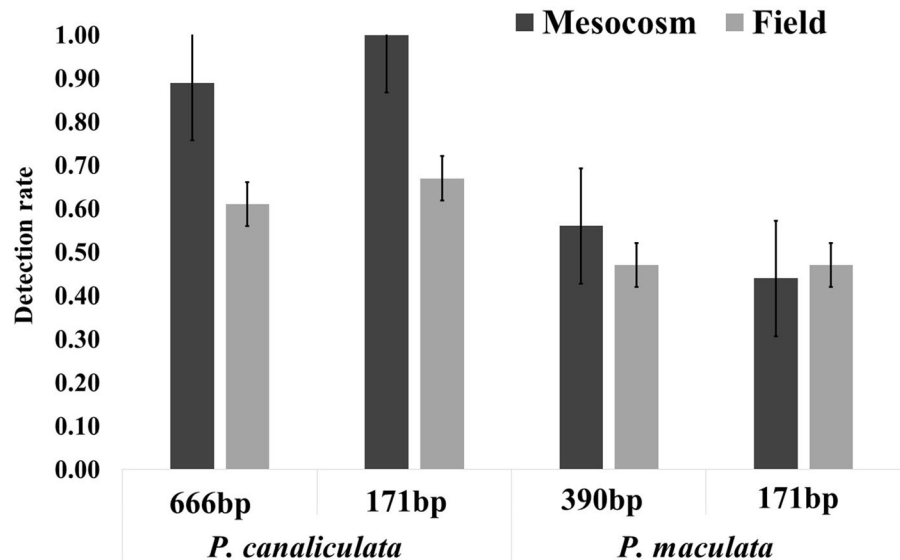
in almost every mesocosm sample (except one sub-sample from aquarium 1) with longer (PcanCOI and HCO2198) and shorter PCR products (POMACF and POMAR) from three aquariums, whereas *P. maculata* was detected 7 out of 9 samples with longer PCR products (PcanCOI and HCO2198) and 5 out of 9 samples with shorter PCR products (POMACF and POMAR). The combined detection rates (using both primers) of *P. canaliculata* and *P. maculata* were 0.94 and 0.50, respectively.

Field validation

The method was validated in 12 sampling locations across four cities in Taiwan (Table 3). Our method successfully detected *Pomacea* spp. from almost every sample in the field (11/12 locations). Both the long and short PCR products were detected equally in the field. *P. canaliculata* and *P. maculata* were detected in all four counties, and in 9 out of 12 sampling sites with long PCR products, and 10 out of 12 sampling sites with shorter PCR products (Table 3). However, we did not amplify any of these species from sampling site CY1. Furthermore, *P. canaliculata* and *P. maculata* were not detected from the site YU1 and CH1, respectively. The combined detection rate (using both primers) of *P. canaliculata* and *P. maculata* of 0.64 and 0.47, respectively (Fig. 7). In our field validation, we also observed a difference in occupancy for both these species, as *P.*

canaliculata was found to be more widespread than *P. maculata*.

Discussion

Mitigating economic and ecological losses caused by invasive species is best achieved via early detection and effective risk assessment (Pyšek & Richardson, 2010; Venette et al., 2021). Therefore, regular monitoring to control their spread, imposing restrictions on their habitat and breeding, and even selective removal approaches or effective utilization can be efficient ways to control invasions (Tobin, 2018). However, the limitations of conventional methods may not allow for efficient and early in-field detection, especially for cryptic species. To overcome these difficulties, we have turned to alternative methods.

Our comparison of the quantitative and qualitative morphological characteristics of two highly invasive and cryptic species, *P. canaliculata*, and *P. maculata*, exhibited difficulties in species diagnosis, which may further present negative knock-on effects for proper ecosystem management. For example, in China, the presence of these two species was only reported after 30 years from their initial introduction, hindering specific management approaches (Yang et al., 2010; Lv et al., 2013). In Taiwan, 40 years have elapsed, since the assumed first introduction of *Pomacea* spp. However, to date, only *P. canaliculata* has been reported

Table 3 Detection rate of *P. canaliculata* and *P. maculata* with eDNA barcoding from rice field located in four different counties of Taiwan

Sampling locations	Sites	Locations	Detection rate of PanCOI, PinsCOI, and HCO2198		Detection rate of POMACF, POMAMF, POMAR	
			P. canaliculata	*P. maculata*	*P. canaliculata*	*P. maculata*
Chiayi	CY1	23° 28′ 44.5″ N 120° 10′ 10.5″ E	0/3	0/3	0/3	0/3
	CY2	23° 27′ 43.3″ N 120° 11′ 39.3″ E	2/3	1/3	2/3	1/3
	CY3	23° 28′ 41.7″ N 120° 12′ 55.8″ E	1/3	1/3	2/3	1/3
Yunlin	YU1	23° 38′ 05.5″ N 120° 12′ 29.9″ E	0/3	3/3	0/3	3/3
	YU2	23° 43′ 36.2″ N 120° 15′ 42.9″ E	3/3	0/3	3/3	1/3
	YU3	23° 46′ 34.8″ N 120° 26′ 04.7″ E	3/3	2/3	2/3	3/3
Changhua	CH1	24° 03′ 37.1″ N 120° 25′ 09.5″ E	2/3	0/3	2/3	0/3
	CH2	24° 09′ 58.5″ N 120° 29′ 36.1″ E	1/3	3/3	2/3	3/3
	CH3	24° 05′ 18.5″ N 120° 35′ 15.3″ E	2/3	1/3	3/3	1/3
Tainan	TA1	23° 12′ 26.1″ N 120° 16′ 15.6″ E	0/3	3/3	2/3	3/3
	TA2	23° 04′ 41.6″ N 120° 18′ 24.8″ E	3/3	1/3	3/3	1/3
	TA3	22° 58′ 43.7″ N 120° 15′ 50.9″ E	3/3	2/3	3/3	1/3

within Taiwan, with *P. maculata* very recently suggested, without definitive evidence. Indeed, previous researchers have reported similar overlapping morphological characters, unable to discriminate between these two species via conventional means (Rama Rao et al., 2018). In the present investigation, we proceed one step further with physicochemical properties through XRD (Leelatawonchai & Laonapakul, 2014; Asimeng et al., 2018; Laonapakul et al., 2019) for the first time (to the best of our knowledge) to distinguish *P. canaliculata* and *P. maculata* using a new and alternative quantitative method, but again found similar chemical compositions. Moreover, while FTIR and Raman spectra are known to be effective in separating other taxon based on their chemical signatures (Rösch et al., 2003; Maity et al., 2013; Yu et al., 2020), no previous research has successfully used these methods to diagnose cryptic species, and in the present study, we were unable to find diagnosable differences between these species. This suggests the need for general methodological refinement or building standard data should researchers and managers wish to implement physicochemical methods for identifying species in the future. The presence of functional groups (–OH, –CO, and –NH; detected through FTIR and Raman analysis) and CaCO$_3$ (conformed through XRD, SEM–EDS) in both snail shells

may indicated a future application on the waste-to-wealth concept of *Pomacea* sp. eradication. Still none of the morphological or physicochemical characters used here are likely to be adopted for species identification by managers or policy regulators. Importantly, because *P. canaliculata* and *P. maculata* are closely related species, they have been suggested to readily hybridize (Matsukura et al., 2008). The evidence of introgressive hybridization of *P. canaliculata* and *P. maculata* in their native and non-native range was recently reported (Glasheen et al., 2020; Yang et al., 2020) which may play a part in their overlapping and indistinguishable characteristics.

Interestingly, results of DNA and eDNA barcoding indicate that these two cryptic species can be putatively separated by simple molecular techniques and confirmed the presence of *P. maculata* (for the first time) along with *P. canaliculata* in Taiwan. The two cryptic species, *P. canaliculata*, and *P. maculata* were effectively amplified by multiplexing species-specific primers PcanCOI (F), PinsCOI (F), and HCO2198 (R) (Fig. 7). The newly designed primers PomaCF, PomaMF, and PomaR were also effective in the sensitive detection of these two species. Although DNA-based barcoding was found to be very effective to identify *Pomacea* spp., it is limited in its field application and may also demonstrate difficulty in

low abundance populations or in early stages of invasion. For example, *P. canaliculata* has recently been reported to have invaded Kenya (Buddie et al., 2021). In such cases, early detection is critical to mitigating their spread prior to widespread establishment. To resolve this problem, the involvement of eDNA-based methods for broad geographical sampling may be more beneficial than the collection and amplification of numerous individuals through DNA barcoding.

Our study successfully standardized and applied eDNA-based methods to detect *P. canaliculata* and *P. maculata* from mixed populations, detecting both the species from semi-natural and natural water bodies. Moreover, both the long and short PCR products were equally detected in both environments (mesocosm and field), suggesting primer choice may be adapted based on information requirements (e.g., longer primers may offer more species-specificity across multiple congeners). Thus, these primers may be the preferable amplification method to detect *Pomacea* invasive species in low abundance. The detection of the presumptive *P. canaliculata*, and *P. maculata* in the same sampling location with eDNA also revealed their syntopic distribution. However, we detected *P. canaliculata* across more sites than *P. maculata*. The difference in detection rate across sampling sites may be due to their uneven geographical distribution, and may also reflect capture bias in heterogeneous environments. However, results demonstrated that eDNA detection was associated with species presence. Our study thus suggests that eDNA methods may be highly applicable in the field and this method can be useful to monitor *Pomacea* spp. in newly introduced places, places of possible introdution, or places where eradication work performed but further confirmation and broadscale sampling across diverse habitats is warranted.

It is importantly to also highlight that the use of eDNA may also present some drawbacks, particularly the inability to detect hybrids without combining nuclear markers (e.g., EF1α) with our COI approach. For example, here we only present the presumed species delineations based on our COI sequences when in effect some samples may represented individuals of mixed ancestry but with *P. maculata* or *P. canaliculata* haplotypes. However, the same restrictions to delineating pure species are also faced with conventional methods. While eDNA has yet to differentiate hybrids for any species (but see Stewart &

Taylor, 2020), particularly through the common use of mtDNA barcodes, future investigations may be able to gain a better understanding of hybrid's impact by developing and using nuclear markers for eDNA. In the present investigation, however, we successfully demonstrated eDNA methods to identify putative *Pomacea* spp. in mesocosms and in the wild for the first time, which remains a pivotal first step and may further provide novel global management approaches for *Pomacea* spp., an exceptionally pernicious invasive organismal group.

Conclusions

In our pioneering study, eDNA-based methods were successfully used in semi-natural and natural water bodies to detect and differentiate (presumed) *P. canaliculata*, and *P. maculata* more accurately than conventional morphological screening. Most importantly, both DNA and eDNA-based methods resolved the long-debated taxonomic confusion of *Pomacea* spp. in Taiwan, and revealed the active presence *Pomacea maculata* in the field. Here, we recommend using eDNA methods over DNA barcoding for these invasive species, particularly for populations in low abundance (e.g., during early invasion or monitoring after eradication), when individual collections are untenable or arduous. However, we suggest the use of nuclear DNA along with mitochondrial DNA to detect the possible occurrence of pure and hybrids lines. Furthermore, quantifying eDNA abundance as a proxy for population density (Lacoursière-Roussel et al., 2016), or the inference of these data for species interactions and their ecological impact remains a critical next step. For example, environmental RNA (eRNA)-based methods could be applied to understand changes of gene expression under different challenging environment, population level interference and species interactions (Yates et al., 2021). Moreover, a detailed understanding of the ecology of *Pomacea* spp. with the help of eDNA and eRNA is warranted to bringing the application of these methods for invasive *Pomacea* spp. mitigation to reality.

Declarations

References

Aitipamula, S. & V. R. Vangala, 2017. X-ray crystallography and its role in understanding the physicochemical properties of pharmaceutical cocrystals. Journal of the Indian Institute of Science 97(2): 227–243.

Asimeng, B. O., J. R. Fianko, E. E. Kaufmann, E. K. Tiburu, C. F. Hayford, P. A. Anani & O. K. Dzikunu, 2018. Preparation and characterization of hydroxyapatite from *Achatina achatina* snail shells: effect of carbonate substitution and trace elements on defluoridation of water. Journal of Asian Ceramic Societies 6(3): 205–212.

Banerjee, P., G. Dey, C. M. Antognazza, R. K. Sharma, J. P. Maity, M. W. Chan, Y.-H. Huang, P.-Y. Lin, H.-C. Chao & C.-M. Lu, 2021. Reinforcement of environmental DNA based methods (Sensu Stricto) in biodiversity monitoring and conservation: a review. Biology 10(12): 1223.

Borromeo, L., N. Egeland, M. Wetrhus Minde, U. Zimmermann, S. Andò, M. V. Madland & R. I. Korsnes, 2018. Quick, easy, and economic mineralogical studies of flooded chalk for EOR experiments using Raman spectroscopy. Minerals 8(6): 221.

Bruce, K., R. C. Blackman, S. J. Bourlat, M. Hellström, J. Bakker, I. Bista, K. Bohmann, A. Bouchez, R. Brys & K. Clark, 2021. A Practical Guide to DNA-Based Methods for Biodiversity Assessment, Pensoft Publishers, Sofia:

Buddie, A. G., I. Rwomushana, L. C. Offord, S. Kibet, F. Makale, D. Djeddour, G. Cafa, K. K. Vincent, A. M. Muvea & D. Chacha, 2021. First report of the invasive snail *Pomacea canaliculata* in Kenya. CABI Agriculture and Bioscience 2(1): 1–10.

Cazzaniga, N. J., 2002. Minireview: old species and new concepts in the taxonomy of Pomacea (Gastropoda: Ampullariidae). Biocell 26: 71.

Chandrashekhar, K., S. Isloor, B. Veeresh, R. Hegde, D. Rathnamma, S. Murag, B. Veeregowda, H. Upendra & N. R. Hegde, 2015. Limit of detection of genomic DNA by conventional PCR for estimating the load of *Staphylococcus aureus* and *Escherichia coli* associated with bovine mastitis. Folia Microbiologica 60(6): 465–472.

Chauhan, A. & P. Chauhan, 2014. Powder XRD technique and its applications in science and technology. Journal of Analytical & Bioanalytical Techniues 5(5): 1–5.

Deiner, K., H. Yamanaka & L. Bernatchez, 2021. The future of biodiversity monitoring and conservation utilizing environmental DNA. Environmental DNA 3(1): 3–7.

Fediajevaite, J., V. Priestley, R. Arnold & V. Savolainen, 2021. Meta-analysis shows that environmental DNA outperforms traditional surveys, but warrants better reporting standards. Ecology and Evolution 11(9): 4803–4815.

Ficetola, G. F., C. Miaud, F. Pompanon & P. Taberlet, 2008. Species detection using environmental DNA from water samples. Biology Letters 4(4): 423–425.

Glasheen, P. M., R. L. Burks, S. R. Campos & K. A. Hayes, 2020. First evidence of introgressive hybridization of apple snails (*Pomacea* spp.) in their native range. Journal of Molluscan Studies 86(2): 96–103.

Harris, J., I. Mey, M. Hajir, M. Mondeshki & S. E. Wolf, 2015. Pseudomorphic transformation of amorphous calcium carbonate films follows spherulitic growth mechanisms and can give rise to crystal lattice tilting. CrystEngComm 17(36): 6831–6837.

Hayes, K. A., R. C. Joshi, S. C. Thiengo, & R. H. Cowie. 2008. Out of South America: Multiple origins of non-native apple snails in Asia. Diversity and Distributions 14(4): 701–712.

Hayes, K. A., R. H. Cowie & S. C. Thiengo, 2009. A global phylogeny of apple snails: Gondwanan origin, generic relationships, and the influence of outgroup choice (Caenogastropoda: Ampullariidae). Biological Journal of the Linnean Society 98(1): 61–76.

Jones, R. R., D. C. Hooper, L. Zhang, D. Wolverson & V. K. Valev, 2019. Raman techniques: fundamentals and frontiers. Nanoscale Research Letters 14(1): 1–34.

Jovanovski, G., V. Stefov, B. Shoptrajanov & B. Boev, 2002. Minerals from Macedonia IV. Discrimination between some carbonate minerals by FTIR spectroscopy. Neues Jahrbuch - Für Mineralogie Abhandlungen. https://doi.org/10.1127/0077-7757/2002/0177-0241.

Kenđel, A. & B. Zimmermann, 2020. Chemical analysis of pollen by FT-Raman and FTIR spectroscopies. Frontiers in Plant Science 11: 352.

Komura, T., H. Kagi, M. Ishikawa, M. Yasui & T. Sasaki, 2018. Spectroscopic Investigation of Shell Pigments from the Family Neritidae (Mollusca: Gastropoda) Biomineralization, Springer, Singapore:, 73–82.

Kupka, T., A. Buczek, M. A. Broda, R. Szostak, H. M. Lin, L. W. Fan, R. Wrzalik & L. Stobiński, 2016. Modeling red coral (*Corallium rubrum*) and African snail (*Helixia aspersa*) shell pigments: Raman spectroscopy versus DFT studies. Journal of Raman Spectroscopy 47(8): 908–916.

Kuzmina, M. L., T. W. Braukmann & E. V. Zakharov, 2018. Finding the pond through the weeds: eDNA reveals underestimated diversity of pondweeds. Applications in Plant Sciences 6(5): e01155.

Lacoursière-Roussel, A., M. Rosabal & L. Bernatchez, 2016. Estimating fish abundance and biomass from eDNA concentrations: variability among capture methods and environmental conditions. Molecular Ecology Resources 16(6): 1401–1414.

Laonapakul, T., R. Sutthi, P. Chaikool, Y. Mutoh & P. Chindaprasirtd, 2019. Optimum conditions for preparation of bio-calcium from blood cockle and golden apple snail shells and characterization. Science 45: 10–20.

Leelatawonchai, P. & T. Laonapakul, 2014. Preparation and characterization of calcium sources from golden apple snail shell for naturally based biomaterials. Advanced Materials Research 931: 370–374.

Liu, C.-C., J. P. Maity, J.-S. Jean, Z. Li, S. Kar, O. Sracek, H.-J. Yang, C.-Y. Chen, A. S. Reza & J. Bundschuh, 2013. The geochemical characteristics of the mud liquids in the Wushanting and Hsiaokunshui Mud Volcano region in southern Taiwan: implications of humic substances for binding and mobilization of arsenic. Journal of Geochemical Exploration 128: 62–71.

Liu, C., Y. Zhang, Y. Ren, H. Wang, S. Li, F. Jiang, L. Yin, X. Qiao, G. Zhang & W. Qian, 2018. The genome of the golden apple snail *Pomacea canaliculata* provides insight into stress tolerance and invasive adaptation. GigaScience 7(9): giy101.

Lowe, S., M. Browne, S. Boudjelas & M. De Poorter, 2000. 100 of the World's Worst Invasive Alien Species: A Selection from the Global Invasive Species Database, Vol. 12. Invasive Species Specialist Group, Auckland:

Lv, S., Y. Zhang, H. X. Liu, L. Hu, Q. Liu, F. R. Wei, Y. H. Guo, P. Steinmann, W. Hu & X. N. Zhou, 2013. Phylogenetic evidence for multiple and secondary introductions of invasive snails: Pomacea species in the People's Republic of China. Diversity and Distributions 19(2): 147–156.

Lv, S., Y.-H. Guo, H. M. Nguyen, M. Sinuon, S. Sayasone, N. C. Lo, X.-N. Zhou & J. R. Andrews, 2018. Invasive Pomacea snails as important intermediate hosts of *Angiostrongylus cantonensis* in Laos, Cambodia and Vietnam: implications for outbreaks of eosinophilic meningitis. Acta Tropica 183: 32–35.

Ma, H., K. Stewart, S. Lougheed, J. Zheng, Y. Wang & J. Zhao, 2016. Characterization, optimization, and validation of environmental DNA (eDNA) markers to detect an endangered aquatic mammal. Conservation Genetics Resources 8(4): 561–568.

Maity, J. P., S. Kar, C.-M. Lin, C.-Y. Chen, Y.-F. Chang, J.-S. Jean & T. R. Kulp, 2013. Identification and discrimination of bacteria using Fourier transform infrared spectroscopy. Spectrochimica Acta Part a: Molecular and Biomolecular Spectroscopy 116: 478–484.

Maity, J. P., P. -R. Ho, Y. -H. Huang, A. -C. Sun, C. -C. Chen, & C. -Y. Chen. 2019. The removal of arsenic from arsenic-bearing groundwater in In-situ and Ex-situ environment using novel natural magnetic rock material and synthesized magnetic material as adsorbent: A comparative assessment. Environmental Pollution 253: 768–778. https://doi.org/10.1016/j.envpol.2019.07.048

Matsukura, K. & T. Wada, 2017. Identification of Pomacea species using molecular techniques. Biology and Management of Invasive Apple Snails, Philippine Rice Research Institute (PhilRice) Maligaya, Science City of Muñoz, Nueva Ecija 3119: 33–43.

Matsukura, K., M. Okuda, K. Kubota & T. Wada, 2008. Genetic divergence of the genus Pomacea (Gastropoda: Ampullariidae) distributed in Japan, and a simple molecular method to distinguish *P. canaliculata* and *P. insularum*. Applied Entomology and Zoology 43(4): 535–540.

McElroy, M. E., T. L. Dressler, G. C. Titcomb, E. A. Wilson, K. Deiner, T. L. Dudley, E. J. Eliason, N. T. Evans, S. D. Gaines & K. D. Lafferty, 2020. Calibrating environmental DNA metabarcoding to conventional surveys for measuring fish species richness. Frontiers in Ecology and Evolution 8: 276.

Naylor, R., 1996. Invasions in agriculture: assessing the cost of the golden apple snail in Asia. AMBIO 25: 443–448.

Ojeda, J. J. & M. Dittrich, 2012. Fourier transform infrared spectroscopy for molecular analysis of microbial cells. In Navid, A. (ed.), Microbial Systems Biology Springer, Cham: 187–211.

Parveen, S., A. Chakraborty, D. K. Chanda, S. Pramanik, A. Barik & G. Aditya, 2020. Microstructure analysis and chemical and mechanical characterization of the shells of three freshwater snails. ACS Omega 5(40): 25757–25771.

Pyšek, P. & D. M. Richardson, 2010. Invasive species, environmental change and management, and health. Annual Review of Environment and Resources 35: 25–55.

Qu, C. & K. A. Stewart, 2019. Evaluating monitoring options for conservation: comparing traditional and environmental DNA tools for a critically endangered mammal. The Science of Nature 106(3): 1–9.

Rama Rao, S., T.-S. Liew, Y.-Y. Yow & S. Ratnayeke, 2018. Cryptic diversity: two morphologically similar species of invasive apple snail in Peninsular Malaysia. PLoS ONE 13(5): e0196582.

Ramos, K., Y. Ang & P. Grootaert, 2020. 'Fake widespread species': a new mangrove Thinophilus Wahlberg (Diptera, Dolichopodidae) from Bohol, Philippines, that is cryptic with a Singaporean species. Raffles Bulletin of Zoology 68: 441–447.

Rawlings, T. A., K. A. Hayes, R. H. Cowie & T. M. Collins, 2007. The identity, distribution, and impacts of non-native apple snails in the continental United States. BMC Evolutionary Biology 7(1): 1–14.

Rösch, P., M. Schmitt, W. Kiefer & J. Popp, 2003. The identification of microorganisms by micro-Raman spectroscopy. Journal of Molecular Structure 661: 363–369.

Shabani, F., M. Ahmadi, L. Kumar, S. Solhjouy-fard, M. S. Tehrany, F. Shabani, B. Kalantar & A. Esmaeili, 2020. Invasive weed species' threats to global biodiversity: future scenarios of changes in the number of invasive species in a changing climate. Ecological Indicators 116: 106436.

Sharma, R. K., S.-C. Wang, J. P. Maity, P. Banerjee, G. Dey, Y.-H. Huang, J. Bundschuh, P.-G. Hsiao, T.-H. Chen & C.-Y. Chen, 2021. A novel BMSN (biologically synthesized mesoporous silica nanoparticles) material: synthesis using a bacteria-mediated biosurfactant and characterization. RSC Advances 11(52): 32906–32916.

Stewart, K. A., & S. A. Taylor. 2020. Leveraging eDNA to expand the study of hybrid zones. Molecular Ecology 29(15): 2768–2776.

Taberlet, P., E. Coissac, M. Hajibabaei & L. H. Rieseberg, 2012. Environmental DNA. Molecular Ecology 21: 1789–1793.

Thiengo, S. C., C. E. Borda & J. Araújo, 1993. On *Pomacea canaliculata* (Lamarck, 1822) (Mollusca; Pilidae: Ampullariidae). Memórias Do Instituto Oswaldo Cruz 88: 67–71.

Tobin, P. C., 2018. Managing invasive species. F1000Research 7: 1686.

Udomkan, N. & P. Limsuwan, 2008. Temperature effects on freshwater snail shells: *Pomacea canaliculata* Lamarck as investigated by XRD, EDX, SEM and FTIR techniques. Materials Science and Engineering: C 28(2): 316–319.

Vagenas, N., A. Gatsouli & C. Kontoyannis, 2003. Quantitative analysis of synthetic calcium carbonate polymorphs using FT-IR spectroscopy. Talanta 59(4): 831–836.

Valand, R., S. Tanna, G. Lawson & L. Bengtström, 2020. A review of Fourier transform infrared (FTIR) spectroscopy used in food adulteration and authenticity investigations. Food Additives & Contaminants: Part A 37(1): 19–38.

Venette, R. C., D. R. Gordon, J. Juzwik, F. H. Koch, A. M. Liebhold, R. K. Peterson, S. E. Sing & D. Yemshanov, 2021. Early Intervention Strategies for Invasive Species Management: Connections Between Risk Assessment, Prevention Efforts, Eradication, and Other Rapid Responses Invasive Species in Forests and Rangelands of the United States, Springer, Cham:, 111–131.

Vrijenhoek, R., 1994. DNA primers for amplification of mitochondrial cytochrome c oxidase subunit I from diverse metazoan invertebrates. Molecular Marine Biology and Biotechnology 3(5): 294–299.

Wu, J.-Y., P.-J. Meng, M.-Y. Liu, Y.-W. Chiu & L.-L. Liu, 2010. A high incidence of imposex in Pomacea apple snails in Taiwan: a decade after triphenyltin was banned. Zoological Studies 49(1): 85–93.

Wu, J.-Y., Y.-T. Wu, M.-C. Li, Y.-W. Chiu, M.-Y. Liu & L.-L. Liu, 2011. Reproduction and juvenile growth of the invasive apple snails *Pomacea canaliculata* and *P. scalaris* (Gastropoda: Ampullariidae) in Taiwan. Zoological Studies 50(1): 61–68.

Yang, Y., Y. Hu, X. Li, X. Wang, X. Mu, H. Song, P. Wang, C. Liu & J. Luo, 2010. Historical invasion, expansion process and harm investigation of *Pomacea canaliculata* in China. Chinese Agricultural Science Bulletin 26: 245–250.

Yang, Q.-Q., S.-W. Liu, C. He & X.-P. Yu, 2018. Distribution and the origin of invasive apple snails, *Pomacea canaliculata* and *P. maculata* (Gastropoda: Ampullariidae) in China. Scientific Reports 8(1): 1–8.

Yang, Q. Q., C. He, G. F. Liu, C. L. Yin, Y. P. Xu, S. W. Liu, J. W. Qiu & X. P. Yu, 2020. Introgressive hybridization between two non-native apple snails in China: widespread hybridization and homogenization in egg morphology. Pest Management Science 76(12): 4231–4239.

Yates, M. C., A. M. Derry & M. E. Cristescu, 2021. Environmental RNA: a revolution in ecological resolution? Trends in Ecology & Evolution 36(7): 601–609.

Yu, S., H. Li, X. Li, Y. V. Fu & F. Liu, 2020. Classification of pathogens by Raman spectroscopy combined with generative adversarial networks. Science of the Total Environment 726: 138477.